EUSIPCO 2013 1569746765

MOTION-BASED INTERPOLATION TO ESTIMATE SPATIALLY VARIANT PSF IN POSITRON EMISSION TOMOGRAPHY

Zacharie Irace, Hadj Batatia

University of Toulouse, IRIT/INP-ENSEEIHT
2, rue Charles Camichel 31071 Toulouse Cedex 7, France

ABSTRACT

This paper deals with the restoration of Positron Emission Tomography images. The partial volume effect creates blurring in such images and causes inaccurate quantization. This artefact is due to the complex geometry of the acquisition system. We propose to represent this complexity by a spatially variable point spread function. The PSF is first measured at a set of locations in the field of view and estimated at any other location. Existing linear interpolation methods consider only the variability of the intensity. In order to consider shape variability of the PSF, we formulate the estimation of an unknown PSF as mass transportation problem of known PSFs. An optimal transport optimization algorithm is used to solve the problem. GATE simulations are used to evaluate the method and compare it to a PCA based approach. Application to partial volume assessment in reconstructed PET images is presented. The promising results set up the possibility to develop more robust PET image restoration.

Index Terms— Partial volume effect, Point Spread Function, PCA, Optimal transport, PET images

1. INTRODUCTION

Positron Emission Tomography (PET) images are used in clinical routine oncology to delineate tumors and quantify their volume and malignity. However, the partial volume effect (PVE) is particularly frequent and severe in this modality [1]. It tends to overestimate the size of tumors and makes their assessment non-precise. It also results in smoothed images that prevent the characterization of heterogeneity of tumors [2]. This phenomenon is mainly due to the complex geometry of the acquisition systems. It has been studied in many fields of research such as astronomy or biological imaging and many techniques of Partial Volume Correction (PVC) have been proposed. In PET imaging, a recent literature review of PVC techniques can be found in [3]. These can be classified into two groups: correction of PVE during image reconstruction, and post-reconstruction techniques. Techniques in the first group often give better results but require processing raw data for reconstruction, which is not feasible in clinical settings. The second group of techniques relies on deconvolution algorithms such as Van-Cittert or Richardson-Lucy that require the impulse response or Point Spread Function (PSF) of the device. Usually, the observed image I is considered as the unknown true image $\hat{I}$ convolved with a Point Spread Function (PSF) h, invariant inside the Field of View (FOV):

$$I = \hat{I} * h \tag{1}$$

However, because of the geometry of the detectors, the PVE behaves significantly differently according to the position within the FOV. The assumption that the PSF is invariant at any point of the FOV leads to poor estimation of the original source. Recent works attempt to remedy this problem by considering spatially variable PSF [4, 5, 6]. Two approaches are commonly used: analytical modeling of the PSF or estimation based on a calibration phase. The estimation consists usually in interpolating the PSF at each position based on the impulse responses measured at a set of few locations in the FOV. Due to the fastidious measurement of source points in the FOV, a coarse grid is often used requiring precise interpolation. In [2], the authors presented a parametric model of the PSF and derived continuous expressions of the parameters based on functions of the radial distance to the center. Non parametric methods which perform better are hindered by the computational time cost of the deconvolution. In astronomy, spatial variability of the PSF has been represented as the linear interpolation of eigen-PSFs obtained by PCA decomposition [5, 7]. However, this technique poses normalization and non-negativity problems [8]. This paper proposes an alternative non-parametric method to estimate the spatially variant PSF at each point of the FOV. The PSF is first measured on a grid of source points. The interpolation of the PSF at any position is formulated as mass transportation problem.

2. METHOD

2.1. Problem statement

Considering the PSF space dependent, the formation of the image I can be modeled by a general case of a Fredholm integral of the first kind:

$$I(x) = \int_{\Omega} \hat{I}(x').h_{x'}(x)dx'. \tag{2}$$

where Ω is the domain of the image. We define the PSF $h_x(.)$ by a vector of coefficients $(h_x(x_1), ..., h_x(x_M))$ where $x_m, m \in \{1 \dots M\}$ are the discrete coordinates of points of a 3-dimensional window centered in x. We consider the PSF known at P locations $\{x_p, p \in [1 \dots P]\}$ on a regular grid in the FOV. For simplicity, we denote $h_p = h_{x_p}$ and $H = h_1, ..., h_p$ the set of known PSFs. The problem is how to estimate $h_x(.)$ at any point x from H. Linear interpolation such as used in PCA-based approaches is appropriate for data that exhibit photometric variability [9]. However, the PSF has also a geometric source of variability which cannot be recovered by linear interpolation even with fine grids. This leads to poor approximations between the reference points.

Geometric-PCA has been investigated in [9]. Given a reference PSF (h_{ref}), the authors compute a family of diffeomorphic deformations that transform h_{ref} into $(h_1, ..., h_P)$. A PCA is performed on the diffeomorphisms, and a PSF h_x is expressed a linear combination of eigen-deformations applied to h_{ref}. This approach ensures that the shape of the PSF evolves continuously within the field of view. However, since elastic deformations are not mass-conservative, the estimated values might not sum to 1 leading to poor approximations. To account for the variability of the shape of the PSF, we express the estimation of the unknown PSF as mass transportation based interpolation.

2.2. Motion-based interpolation

The proposed motion-based interpolation relies on a mass transport problem, known as the *Monge-Kantorovich* problem [10, 11]. Its resolution gives the optimal way to displace one reference PSF h_{ref} to any other PSF h_x, while conserving its mass (values sum to 1).

The motion-based interpolation method presented here is inspired by the two-point method developed in [12]. It consists in four steps. First, each known PSF (h_p) is expressed as a mixture of Gaussians $G_{\mu_{p,i},\sigma_{p,i}}(x)$, called particles each having a weight $w_{p,i}$ called mass. And one PSF is chosen as reference (h_{ref}). Second, a mass transport registration is performed between each (h_p) and (h_{ref}). This results in mapping each particle of mass $w_{ref,i}$ to several particles of masses $\{w_{p,j}\}$ with partial-masses $w_p^{i \to j}$. Third, we rewrite the mixture of Gaussians for all known PSFs in order to have a set of identical masses $\{q_{i1}, ..., q_{iN}\}$ for every particle i. The estimation of an unknown PSF at the location x is then done by interpolating the parameters of the Gaussians corresponding to identical masses and summing to compute its coefficients. These steps are detailed in the following sub-sections.

2.2.1. Particle decomposition

In order to capture the variability of the shape of the PSF, we consider any PSF h_p as a mixture of Gaussian functions:

$$h_p(x) = \sum_i w_{p,i} G_{\theta_{p,i}}(x) \tag{3}$$

Each term is considered a particle characterized by its weight $w_{p,i}$ and shape $\theta_{p,i} = (\mu_{p,i}, \sigma_{p,i})$. The decomposition can be achieved using a non-negative least-squares formulation[12]:

$$\arg\min_{w_{p,i}} \sum_m [h_p(x_m) - \sum_i w_{p,i} G_{\theta_{p,i}}(x_m)]^2 \tag{4}$$

2.2.2. Mass transport registration

Let h_{ref} be one PSF chosen as reference among $h_1, ..., h_P$. We consider the registration problem that expresses the transformations mapping each h_{ref} onto h_p. In order to ensure continuous evolution of the shape of the PSF, we formulate the registration as a mass transportation problem. The underlying idea is to displace continuously each particle $h_{ref,i} = w_{ref,i} G_{\theta_{ref,i}}$ to $h_{p,j} = w_{p,j} G_{\theta_{p,j}}$. This leads to continuous evolution of θ along the path taken during the transportation. Solving the mass transportation problem is achieved by optimizing the *Earth Mover's Distance* (EMD) between $h_{ref,i}$ and $h_{p,j}, \forall (i,j)$:

$$\begin{cases} \hat{w}_p^{i \to j} = \arg\min_{w_p} \sum_i \sum_j c_{i,j} w_p^{i \to j}; \text{ with} \\ h_{ref,i} = \sum_j w_p^{i \to j} G_{\theta_{ref,i}} \\ h_{p,j} = \sum_i w_p^{i \to j} G_{\theta_{p,j}} \end{cases} \tag{5}$$

where $c_{i,j}$ is a known cost to move one unit from $\mu_{\text{ref},i}$ to $\mu_{p,j}$. Precisely, $c_{i,j}$ corresponds to their Euclidian distance and $w_p^{i \to j}$ is the unknown *quantity* to be moved from $\mu_{\text{ref},i}$ to position $\mu_{p,j}$. This optimization problem is solved using a network simplex method [12]. As a result, we can write:

$$h_p(x) = \sum_j \sum_i w_p^{i \to j} G_{\theta_{p,j}}(x) \tag{6}$$

2.2.3. Multi-point interpolation

The resolution of the previous mass transport problem causes each particle composing the reference h_{ref} to be paired with one or more particles in the target distributions h_p, in such a way that:

$$\forall i, \forall p, w_{\text{ref},i} = \sum_j w_p^{i \to j} \tag{7}$$

Based on this, the aim of the multi-point interpolation phase is to estimate the PSF at any location. We define a set of weights $Q^i = \{q_{i,1}, ..., q_{i,N}\}$ and $Q^i_{p,j} \subset Q^i$ a subset of Q^i, so that:

$$\begin{cases} w_p^{i \to j} = \sum_{q \in Q^i_{p,j}} q; \forall i, \forall j, \forall p, \text{and} \\ w_{\text{ref},i} = \sum_{q \in Q^i} q \end{cases} \tag{8}$$

Intuitively, this decomposition consists in splitting the particles in such a way that each particle composing h_{ref} matches a unique particle *of the same mass* in each target distributions h_p. The algorithm 1 describes the process of splitting the particles to construct the set of masses Q^i.

Algorithm 1 Particle splitting

Initialization

$\forall i, Q^i \leftarrow \emptyset$

$\forall i, j, p, Q^i_{p,j} \leftarrow \emptyset$

$\forall i, j, p, \tilde{w}_p^{i \to j} \leftarrow w_p^{i \to j}$

$n \leftarrow 1$

For each particle of the origin

for all i **do**

  repeat

Find the heaviest particle for each p and the associated j

    $\forall p, \tilde{w}_p^{\max} \leftarrow \max_j \tilde{w}_p^{i \to j}$

    $J_{\max} \leftarrow \{\operatorname{argmax}_j \tilde{w}_p^{i \to j}\}_p$

Create the new particle

    $q_{i,n} \leftarrow \min_p \tilde{w}_p^{\max}$; $n \leftarrow n + 1$

    $Q^i \leftarrow Q^i \cup \{q_{i,n}\}$

    $\forall p, \forall j \in J_{\max}, Q^i_{p,j} \leftarrow Q^i_{p,j} \cup \{q_{i,n}\}$

Subtract the mass

    $\forall p, \forall j \in J_{\max}, \tilde{w}_p^{\max} \leftarrow \tilde{w}_p^{\max} - q_{i,n}$

  until $q_{i,n} < 0.0001$

end for

Now, a given particle of mass q is associated to specific parameter $\theta_{p,k} = (\mu_{p,k}, \sigma_{p,k})$ at each location p of the learning set. It is then easy to interpolate this pair of parameters (μ_x and σ_x) to estimate the behavior of the particle at any position x of the FOV. Having obtained the resulting coordinates for each particle, and knowing their mass, the PSF at any point h_x can finally be reconstructed as the sum of these particles.

3. APPLICATION TO PET IMAGES

3.1. Data simulation

Experiments have been conducted on a simulated GE Discovery ST PET/CT 3D scanner using the software *GATE* [13]. Because of the scanners tangential symmetry, we considered that the PSF is characterized by its center at axial and radial position (ρ, z) and varies in the 3D space $(\vec{\rho}, \vec{z}, \vec{\varphi})$. The PSF that are not located in the plane $\varphi = 0$ are obtained by a rotation of φ after estimating the corresponding PSF in the plane. During the learning phase, a set of source points (hereafter called learning set) have been positioned at different radii and depth from the scanner's center, on a regular grid, at radial distances: 0, 70, 140, 210 and 280 mm and at axial positions 0, 15, 30, 45, and 60 mm. This configuration allows covering all the possible shapes of the PSF. The source points have been modeled by a 0.1mm radius sphere with a $100'000$ becquerels activity during an exposition of 30 minutes. The images of each source point have been reconstructed by an MLEM algorithm (10 iterations) [14], without blurring filter, in order to preserve the data statistics. The size of the reconstructed image was set to $256 \times 256 \times 48$ pixels.

3.2. Results of the PCA

A PSF basis was calculated by applying PCA on the learning set. Figure 1 shows the normalized cumulative variance according to the number eigen-vectors K kept in the basis. One

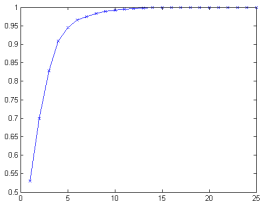

Fig. 1. Normalized cumulative variance

can see that 6 eigen-vectors are sufficient to model 95% of the variability of the PSF, and 10 to cover 99% of the variance.

The coefficients associated to the first 4 eigen-PSF, through the plane (ρ, z), are displayed in figure 2 . As

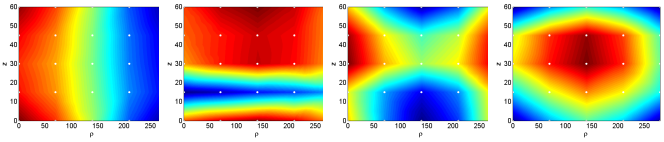

Fig. 2. Coefficients associated to the first 4 eigen-PSF in the plane $(\vec{\rho}, \vec{z})$ (The white dots are the positions of the learning set).

expected, the variability of the PCA mainly occurs along the radial direction $\vec{\rho}$. The variance of the PSF's shape does not vary significantly in the axial direction $\vec{z}$ because the axial configuration of the scanner is symmetric, except for the positions that are subject to border effect. At last, one notice that for some directions (e.g. third component), the coefficients are not regular, justifying the use of another type of interpolation in which the coefficients are more regular.

3.3. Partial Volume Effect retrieval

The aim of these experiments was to compare the retrieval of the PSF at any location of the FOV. A set of 41 source points have been generated at random positions inside the FOV. The reconstructed images have been cropped and compared to PSF estimated from 3 approaches:

- A spatially invariant PSF h_{ref}.

- A spatially variant PSF, based on the PCA decomposition $h_{\text{pca}}(x)$, as presented in [5, 7].
- A spatially variant PSF, based on mass transportation $h_{\text{mt}}(x)$, as explained in **??**.

Note that h_{ref} used in the first method is the same as the reference PSF used in the motion-based interpolation method.

The Euclidian distances between the measured and estimated images has been computed, and summed over the 41 testing set. The results are presented in table 1. The

Method	Sum of the distances
Spatially invariant PSF (h_{ref})	4.79
PCA-based method (h_{pca})	2.63
Mass transportation-based (h_{mt})	0.67

Table 1. Sum of the Euclidian distances between the measured and estimated images of the testing set

motion-based interpolation offers by far the best results. As expected, the use of the spatially-variant h_{pca} is still better than the spatially-invariant h_{ref}.

Figure 3 shows an example of a 2D-slice of the measured PSF, and its corresponding estimations from the three approaches. One sees that the PSF h_{pca} obtained from the lin-

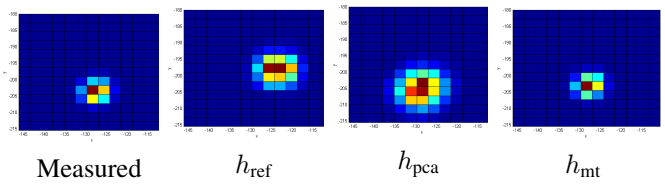

Fig. 3. Measured PSF and estimations from the three methods.

ear interpolation method is more spread than the other PSF. That comes from the fact that the estimated PSF h_{pca} is expressed as a mixture of PSFs obtained from the learning set that may not aligned one to another.

4. CONCLUSION

This paper presented a mass transport based method to estimate a spatially variable PSF from a learning set. The method consists in expressing the PSF as a mixture of Gaussians, or particles. The weights or masses of each mixture of a known PSF are registered to a reference PSF. The resulting weights serve to rewriting the mixture in order to have identical masses for every particle. The estimation of the PSF at a any position becomes the mixture of interpolated Gaussians corresponding to identical masses. Experiments have been conducted on GATE data simulated for a General Electric PET/CT acquisition system. Comparison with a PCA-based approach show very significantly better results to our method.

Future work will concentrate on fast deconvolution methods based on our representation of the PSF in a similar way to [5] for PCA-based deconvolution. The idea is to speed up the convolution based on the fact that our PSF is a sum of gaussians, that can be seen as separable kernels. Another perspective concerns integrating this method in a blind deconvolution approach.

5. REFERENCES

[1] Marine Soret, Stephen L. Bacharach, and Irene Buvat, "Partial-volume effect in pet tumor imaging," *J Nucl Med*, vol. 48, no. 6, pp. 932–945, 2007.

[2] David L Barbee, Ryan T Flynn, James E Holden, Robert J Nickles, and Robert Jeraj, "A method for partial volume correction of pet-imaged tumor heterogeneity using expectation maximization with a spatially varying point spread function," *Physics in Medicine and Biology*, vol. 55, no. 1, pp. 221, 2010.

[3] Kjell Erlandsson, Irene Buvat, P Hendrik Pretorius, Benjamin A Thomas, and Brian F Hutton, "A review of partial volume correction techniques for emission tomography and their applications in neurology, cardiology and oncology," *Physics in medicine and biology*, vol. 57, no. 21, pp. R119, 2012.

[4] James G. Nagy and Dianne P. O'Leary, "Fast iterative image restoration with a spatially varying psf," *Advanced Signal Processing: Algorithms, Architectures, and Implementations VII*, vol. 3162, pp. 388–399, 1997.

[5] Tod Lauer, "Deconvolution with a spatially-variant psf," *Astronomical Data Analysis II*, vol. 4847, pp. 167–173, 2002.

[6] David Miraut and Javier Portilla, "Efficient shift-variant image restoration using deformable filtering (part i)," *EURASIP Journal on Advances in Signal Processing*, vol. 2012, no. 1, pp. 1–20, 2012.

[7] M. J. Jee, J. P. Blakeslee, M. Sirianni, A. R. Martel, R. L. White, and H. C. Ford, "Principal component analysis of the time- and position-dependent point-spread function of the advanced camera for surveys," *Publications of the Astronomical Society of the Pacific*, vol. 119, no. 862, pp. pp. 1403–1419, 2007.

[8] Ron Zass and Amnon Shashua, "Nonnegative sparse pca," in *In Neural Information Processing Systems*, 2007.

[9] Jérémie Bigot, Raul Gouet, and Alfredo Lopez, "Geometric pca of images," Tech. Rep., Institut de Mathématiques de Toulouse - IMT , Centre de modélisation mathématique - CMM, Feb. 2012.

[10] Gaspard Monge, *Mémoire sur la théorie des déblais et des remblais*, De l'Imprimerie Royale, 1781.

[11] L.V. Kantorovich, "On a problem of monge," *Uspekhi Mat. Nauk*, vol. 3, pp. 225–226, 1948.

[12] Nicolas Bonneel, Michiel van de Panne, Sylvain Paris, and Wolfgang Heidrich, "Displacement interpolation using lagrangian mass transport," *ACM Trans. Graph.*, vol. 30, no. 6, pp. 158:1–158:12, Dec. 2011.

[13] S Jan, G Santin, D Strul, S Staelens, K Assi, D Autret, S Avner, R Barbier, M Bardis, P M Bloomfield, D Brasse, V Breton, P Bruyndonckx, I Buvat, A F Chatziioannou, Y Choi, Y H Chung, C Comtat, D Donnarieix, L Ferrer, S J Glick, C J Groiselle, D Guez, P-F Honore, S Kerhoas-Cavata, A S Kirov, V Kohli, M Koole, M Krieguer, D J van der Laan, F Lamare, G Largeron, C Lartizien, D Lazaro, M C Maas, L Maigne, F Mayet, F Melot, C Merheb, E Pennacchio, J Perez, U Pietrzyk, F R Rannou, M Rey, D R Schaart, C R Schmidtlein, L Simon, T Y Song, J-M Vieira, D Visvikis, R Van de Walle, E Wiers, and C Morel, "Gate: a simulation toolkit for pet and spect," *Physics in Medicine and Biology*, vol. 49, no. 19, pp. 4543, 2004.

[14] L.A. Shepp and Y. Vardi, "Maximum likelihood reconstruction for emission tomography," *Medical Imaging, IEEE Transactions on*, vol. 1, no. 2, pp. 113–122, 1982.